Multi-scale complexity entropy causality plane: An intrinsic measure for indicating two-phase flow structures*

Dou Fu-Xiang(窦富祥)[a], Jin Ning-De(金宁德)[a]†, Fan Chun-Ling(樊春玲)[a], Gao Zhong-Ke(高忠科)[a], and Sun Bin(孙 斌)[b]

[a] School of Electrical Engineering and Automation, Tianjin University, Tianjin 300072, China
[b] College of Metrological and Engineering, China Jiliang University, Hangzhou 310018, China

(Received 7 May 2014; revised manuscript received 15 July 2014; published online 10 October 2014)

We extend the complexity entropy causality plane (CECP) to propose a multi-scale complexity entropy causality plane (MS-CECP) and further use the proposed method to discriminate the deterministic characteristics of different oil-in-water flows. We first take several typical time series for example to investigate the characteristic of the MS-CECP and find that the MS-CECP not only describes the continuous loss of dynamical structure with the increase of scale, but also reflects the determinacy of the system. Then we calculate the MS-CECP for the conductance fluctuating signals measured from oil–water two-phase flow loop test facility. The results indicate that the MS-CECP could be an intrinsic measure for indicating oil-in-water two-phase flow structures.

Keywords: oil–water two-phase flow, fluid dynamics, complexity entropy, multi-scale

PACS: 05.45.–a, 05.45.Tp, 47.52.+j, 47.11.St **DOI:** 10.1088/1674-1056/23/12/120502

1. Introduction

Two-phase flow is regarded as a nonlinear dynamic system with complex characteristics of chaos and dissipation,[1–5] and the flow behavior presents high irregularity and structural diversity. The distribution of two phases, i.e., flow structure, affects the flow pressure loss and heat and mass transfer characteristics of the two-phase flow, which has a great influence on the accurate measurement of the flow characteristic parameters. Therefore, the identification of the flow structure has become one of the key problems in the study of two-phase flow. Recently, many methods have been applied to two-phase flow analysis, including numerical simulation,[6–8] experimental measurement,[9–12] power spectrum analysis,[13,14] and nonlinear analysis.[15–18] Especially, entropy, as an important parameter to characterize complexity, has been proved to be a powerful tool for identifying the two-phase flow. For instance, Zheng and Jin[19] proposed the multi-scale sample entropy (MSSE) to classify different flow patterns of gas–liquid two-phase flow. Fan *et al.*[20] employed the multi-scale permutation entropy (MSPE) in detecting the dynamical complexity of different flow conditions. These methods provide a novel way of identifying flow patterns from the perspective of complexity measure. Accordingly, seeking a complexity measure to indicate the complexity of internal dynamic structure of two-phase flow can be of great help in uncovering the flow characteristic of two-phase flow.

Based on the probabilistic description of a physical system, a family of statistical complexity measures[21–23] has been proposed. The members of this family purport to ascertain the degree of periodicity and randomness of a system. In particular, Rosso *et al.*[24] proposed a representation called the complexity entropy causality plane (CECP). Its horizontal and vertical axes are the permutation entropy and the intensive statistical complexity measure, describing the complexity of a system in the respect of "information" and "disequilibrium". Compared with the permutation entropy, the CECP provides additional information regarding the peculiarities of a probability distribution. This method is very promising to distinguish between a chaotic system and stochastic process, and it has been applied to financial data analysis,[25] commodity market analysis,[26] the music classification,[27] etc. However, it is worth mentioning that the complexity of a system cannot be measured univocally, because it also depends on the scale of observation. In this regard, according to the complexity entropy causality plane (CECP), we propose the multi-scale complexity entropy causality plane (MS-CECP), and further we use it to characterize different flow behaviors underlying oil-in-water two-phase flows.

2. Statistical complexity measure

Before the discovery of chaos, physical processes were broadly described in terms of two extreme models of behaviors: period and random.[28,29] These two processes are both simple, but in distinct senses: period is temporally repetitive so that its probability distribution is centered around some prevailing states; random affords a compact statistical description

*Project supported by the National Natural Science Foundation of China (Grant Nos. 41174109 and 61104148), the National Science and Technology Major Project of China (Grant No. 2011ZX05020-006), and the Zhejiang Key Discipline of Instrument Science and Technology, China (Grant No. JL130106).

†Corresponding author. E-mail: ndjin@tju.edu.cn

© 2014 Chinese Physical Society and IOP Publishing Ltd

that can achieve any of its accessible states with the same probability. As two kinds of complexity measures, "information" and "disequilibrium" describe the complexity of a system from different perspectives: "information" shows the amount of information needed for describing the behavior of the system; "disequilibrium" obtains the distance between a given probability distribution and the equilibrium probability distribution. For the two simple processes, period has lower "information" and higher "disequilibrium", while random has higher "information" and lower "disequilibrium". In this regard, neither "information" nor "disequilibrium" can give the same description of the complexity for the two simple processes.

In view of the characteristics stated above, Lopez–Ruiz *et al.*[21] proposed a measure of complexity by relating "information" to "disequilibrium". This measure of complexity vanishes for the perfect order process and maximal randomness process, and in between these two extremes there exists a wide range of possible degrees of physical structures. Based on this kind of complexity measure, a class of statistical complexity measure has been proposed, such as LMC (Lopez–Ruiz, Mancini and Calbet) measure,[21] SDL (Shiner, Davison and Landsberg) measure,[30] and the complexity measure $C_{\rm JS}$.[22–24] The members of this family purport to detect the intricate structures behind the dynamics and ascertain the degree of unpredictability and randomness of a system.[22]

The complexity measure $C_{\rm JS}[P]$ proposed by Rosso *et al.*[24] is a function of the probability distribution P associated with the time series. $C_{\rm JS}[P]$ is defined as

$$C_{\rm JS}[P] = Q_{\rm J}[P,P_{\rm e}]H_{\rm S}[P], \tag{1}$$

where $Q_{\rm J}[P,P_{\rm e}]$ is the normalized Jensen–Shannon divergence, and $H_{\rm S}[P]$ is the normalized Shannon's entropy.

For a given time series $\{x(t)\}_{t=1}^{N}$, we can obtain a reconstructed vector $X(i)$ by embedding the time series in an m-dimensional space

$$\begin{aligned} X(i) &= [x(i), x(i+\tau), \ldots, x[i+(m-1)\tau]], \\ i &= N-(m-1)\tau, \end{aligned} \tag{2}$$

where m is the embedding dimension and τ is the embedding time delay. For each of these vectors, we arrange the permutation $\pi = [j_0, j_1, \ldots, j_{m-1}]$ of $[0,1,\ldots,m-1]$ defined by $x[i+(j_0-1)\tau] \le x[i+(j_1-1)\tau] \le \cdots \le x[i+(j_{m-1}-1)\tau]$. Consider that $j_{s-1} < j_s$ if $x[i+(j_{s-1}-1)\tau] = x[i+(j_s-1)\tau]$ so as to obtain a unique result. Therefore, for all $m!$ possible permutations of π, the probability distribution $P = \{p(\pi_k), k = 1,\ldots,m!\}$ is given by

$$p(\pi_k) = \frac{\#\{X(i) | i \le N-(m-1)\tau;\ \ X(i) \text{ has type } \pi_k\}}{N-(m-1)\tau}, \tag{3}$$

where # denotes the occurrence frequency of the permutation type π. Thus, the normalized Shannon's entropy is given by

$$H_{\rm S}(P) = S(P)/\ln(m!), \tag{4}$$

where $S[P] = -\sum_{k=1}^{m!} p(\pi_k)\ln(p(\pi_k))$ is the standard Shannon's entropy.

The embedding dimension m and the time delay τ play an important role in calculating the appropriate probability distribution. In particular, Bandt and Pompe[31] suggested the dimension $3 \le m \le 7$ and the time delay $\tau = 1$ for practical purposes. In the present work, we use $m = 6$ based on the false nearest neighbors (FNNs)[32] and $\tau = 1$. Moreover, it is necessary to ensure the length of the time series $N \ge m!$ in order to achieve a reliable statistic.

Jensen–Shannon divergence is a method of measuring the similarity between two probability distributions. It obtains the distance between the probability distribution $P = \{p(\pi_k), k = 1,\ldots,m!\}$ and the equilibrium probability distribution $P_{\rm e} = \{p_k = 1/m!; k = 1,\ldots,m!\}$, which describes the disequilibrium of the probability distribution. The Jensen–Shannon divergence $Q_{\rm J}[P,P_{\rm e}]$ reads

$$Q_{\rm J}[P,P_{\rm e}] = Q_0\{S[(P+P_{\rm e})/2] - S[P]/2 - S[P_{\rm e}]/2\}, \tag{5}$$

where Q_0 is a normalization constant, and its value is

$$Q_0 = -2\left\{\left(\frac{m!+1}{m!}\ln(m!+1) - 2\ln(2m!) + \ln(m!)\right)\right\}^{-1}. \tag{6}$$

The complexity measure $C_{\rm JS}$ provides additional information that cannot be reflected by the permutation entropy. Moreover, it can quantify the degree of structural correlations and detect intricate structures or patterns behind the dynamics. Since the opposite extremes of perfect order process and maximal randomness process contain neither nontrivial nor complex structures, they are defined to have zero statistical complexity.

In order to study the time evolution characteristics of $C_{\rm JS}$, Rosso *et al.*[24] proposed a representation space called complexity entropy causality plane (CECP), with its horizontal and vertical axis being the normalized permutation entropy $H_{\rm S}$ and the complexity measure $C_{\rm JS}$, respectively.

3. Complexity entropy causality plane

We analyze three different classes of signals: (a) periodic process (PP), (b) chaotic system (CS), and (c) stochastic process (SP) as illustrative examples, in order to study the ability to recognize different types of signals in the CECP.

(i) The sine signal $x = \sin(0.3\pi t)$ is chosen as a kind of PP, and the sampling interval is selected to be 0.01.

We select the following five kinds of CSs:

(ii) Logistic map:

$$x_{n+1} = r x_n(1-x_n), \tag{7}$$

where the value $r = 4$ and the initial value $x_0 = 0.512$.

(iii) Henon map:

$$\begin{cases} x_{n+1} = 1 - ax_n^2 + y_n, \\ y_{n+1} = bx_n, \end{cases} \tag{8}$$

where $a = 1.4$, $b = 0.3$, and the initial value $(x_0, y_0) = (0.1, 0.1)$. In particular, we take x variable for analysis.

(iv) Skew tent map:

$$\begin{cases} x/\omega, & x \in (0, \omega), \\ (1-x)/(1-\omega), & x \in (\omega, 1), \end{cases} \tag{9}$$

where we use the value $\omega = 0.1847$.

(v) Lorenz system:

$$\begin{cases} \dot{x} = s(y - x), \\ \dot{y} = rx - y - xz, \\ \dot{z} = xy - bz, \end{cases} \tag{10}$$

where $s = 16$, $r = 45.92$, $b = 4$ and the initial value $(x_0, y_0, z_0) = (-1, 0, 1)$. In particular, we only use x-values for analysis.

(vi) Schuster maps: a class of maps that display laminar regions separated by chaotic bursts as

$$x_{n+1} = x_n + x_n^z, \quad \mod 1, \tag{11}$$

the size of laminar region reduces with the decrease of z, making the system close to a fully chaotic system and more complex. The initial values are $x_0 = 0.05$ and $z = 2.5$, 2, 1.5, respectively.

(vii) Noises with f^{-k} power spectrum (k-noise),[24] which are selected as a kind of SP: for different k values, the k-noises exhibit different random characteristics.

For all the cases the length of time series we study here is 4×10^4, meeting the condition $N \geq m!$. The results of both H_S and C_{JS} are plotted in Fig. 1.

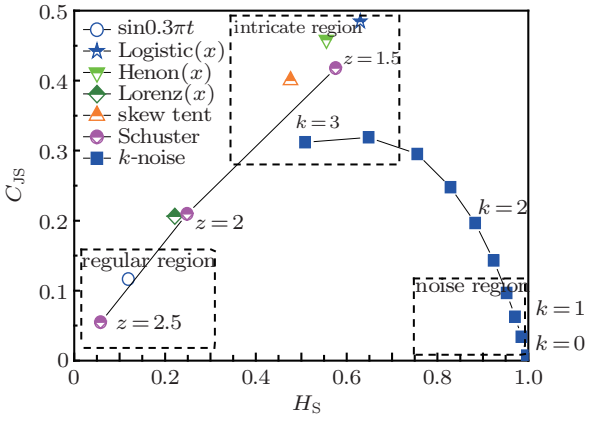


Fig. 1. (color online) CECPs for several typical dynamic systems.

As shown in Fig. 1, the result of the sine signal is located in the lower left of the plane, near to the coordinate point $(0.1, 0.1)$. The low values of H_S and C_{JS} are consistent with the low complexity and regular structure of sine signal. In this way, we name this area the regular region (R-region).

For the discrete chaotic system, i.e., the Logistic map, the Henon map, and the skew tent map, the results in Fig. 1 show that 1) H_S is situated between 0.4 and 0.7, 2) C_{JS} is located between 0.4 and 0.5, near to the maximum value. Higher C_{JS} and H_S values are caused by intricate structures immersed in the CS. Therefore, we name this region the intricate region (I-region). As for the continuous chaotic system, the Lorenz system obtains relatively low C_{JS} and H_S values compared with the other CSs. The Schuster maps exhibit different chaotic degrees, depending on the z value. As shown in Fig. 1, for different z values, Schuster maps are located at three different points in the CECP. The less the value z, the higher the values of C_{JS} and H_S will be. The results show that the CECP is an effective tool for quantifying different chaotic degrees of chaotic systems.

For the k-noises with $0 < k < 3$, the H_S values are in a range from 0.5 to 1, while the C_{JS} values range from 0.35 to 0. With the increase of k, the correlations between consecutive points in the time series become obvious and, accordingly, H_S decreases. In particular, for smaller k values: $k = 0$ and $k = 1$, the k-noises almost become ideal noises, with $H_S \approx 1$ related to its irregular and unpredictable characteristic and $C_{JS} \approx 0$, for it does not contain any non-trivial structures. In this regard, we name this area the noise region (N-region). Obviously, the CECP can quantify the degrees of randomness for different colored noises.

Consequently, the CECP can measure the complexity induced by the correlational structures and distinguish different classes of signals, where chaos and noise are located at different positions. Such a representational property could be useful to analyze the real data which are always mixed with omnipresent noise.

4. Multi-scale complexity entropy causality plane for typical systems

In Fig. 1, the point of the Lorenz system is close to that of the Schuster map with $z = 2$, but the dynamic characteristics of the two systems are different from each other. In this regard, the CECP has its limitation in revealing dynamical characteristics with a single scale. To better understand the dynamic characteristics of a system, we combine the CECP with the multi-scale technique,[33] yielding MS-CECP.

The method of the multi-scale technique is described as follows: for a given time series $\{x(t), t = 1, 2, \ldots, N\}$, reconstruct it with the scale s and obtain the coarse grained time

series $\{y^s(j), j = 1,2,\ldots,N/s\}$ which is generated by

$$y^s(j) = \frac{1}{s} \sum_{t=(j-1)s+1}^{js} x(t), \quad 1 \le j \le N/s. \tag{12}$$

Obviously, the obtained coarse-grained time series is the original time series when the scale is 1.

Here, we take sine signal, Logistic signal, Lorenz signal, Schuster maps with $z = 2.5$, 2, 1.5, as well as k-noise with $k = 0$ for example to analyze the dynamics of the MS-CECP, and select the maximum scale to be 60.

Before multi-scale analysis, it is necessary to take into account the effect of the length of time series on the calculated results. According to Eq. (12), the length of coarse-grained time series reduces with increasing the scale. However, to make the probability distribution work with a reliable statistic, we should ensure that the length of the time series meets the condition $N \ge m!$. In this regard, we examine the results for different sequence lengths, with the original signal lengths of 1×10^4, 5×10^4, 1.0×10^5, 1.5×10^5, and 2.0×10^5, respectively (see Fig. 2).

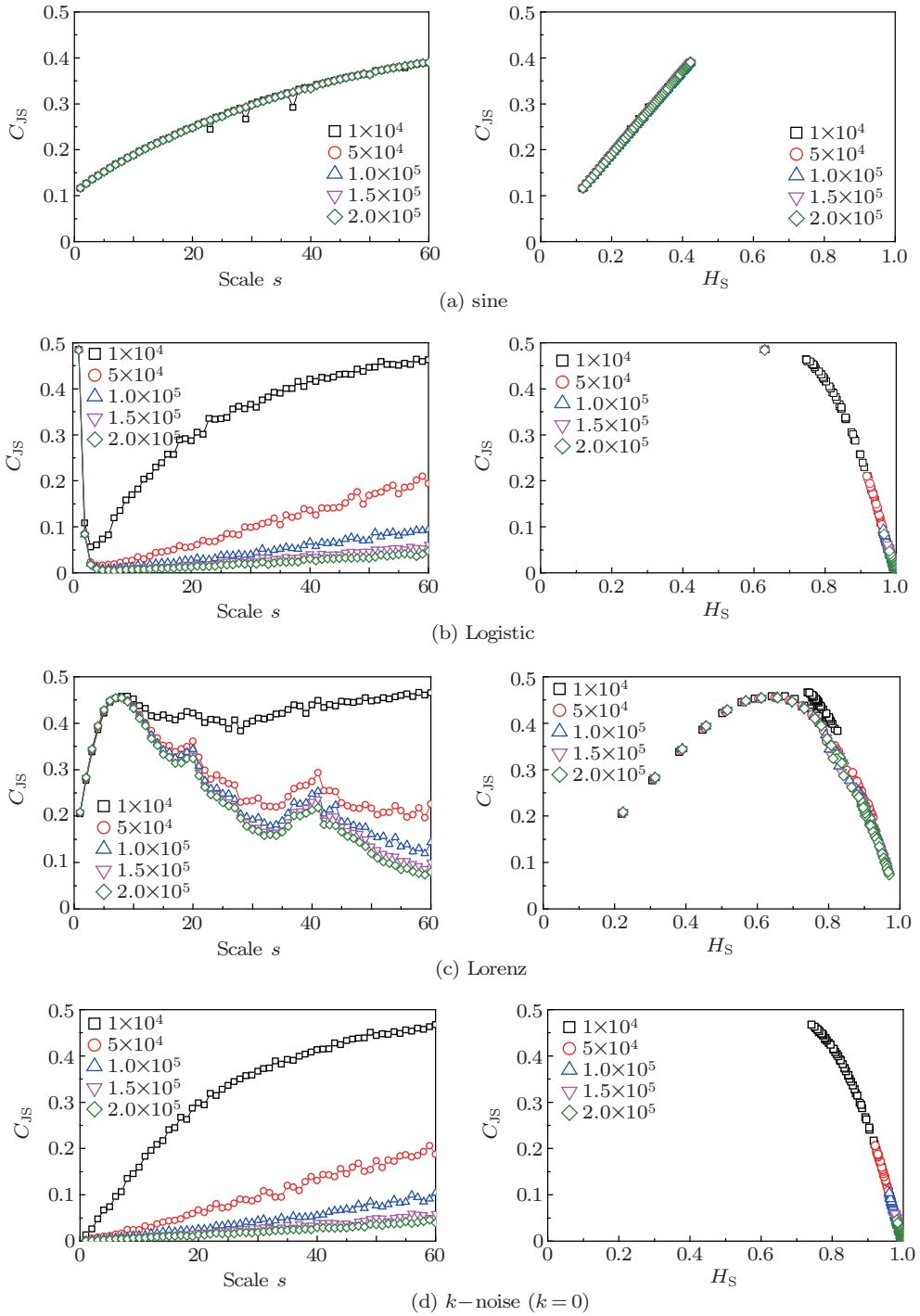


Fig. 2. (color online) MS-CECPs for four typical systems, with the original sequence lengths of 1×10^4, 5×10^4, 1.0×10^5, 1.5×10^5, and 2.0×10^5 respectively: (a) sine signal; (b) Logistic signal; (c) Lorenz signal; (d) k-noise ($k = 0$).

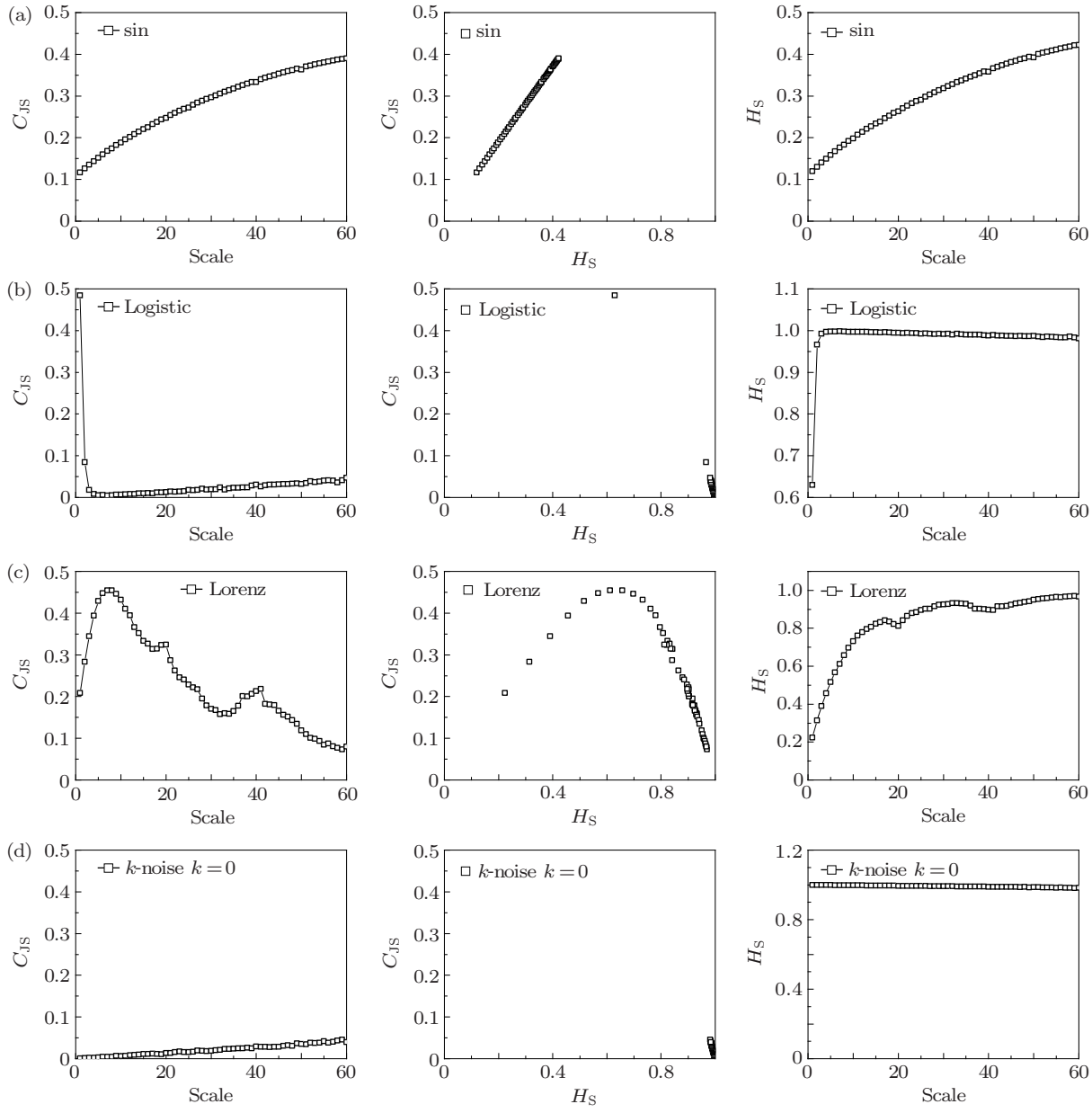


Fig. 3. C_{JS} and H_S versus scale, and MS-CECPs for four typical systems with the sequence length of 2.0×10^5: (a) sine signal; (b) Logistic signal; (c) Lorenz signal; (d) k-noise ($k = 0$).

For all systems in Fig. 2, the results for different sequence lengths diverge more notably as the points move into the lower right of the MS-CECP (N-region). The reason for such a behavior is that the probability distribution is close to the stochastic distribution for the point near the N-region. However, stochastic distribution requires a large number of data as a support to show its random feature, in this way the length of sequence has a greater influence on the calculated results. Meanwhile, for the sine signal and the Lorenz signal, we can see that the sequence length of 5×10^4 can afford a relatively accurate result, and the length of the coarse-grained time series meets the condition $N > m! = 720$ when the scale is up to 60. To better reflect the dynamic characteristics of MS-CECP, we select sequence length of 2×10^5. The MS-CECPs for sine, Logistic, Lorenz signals, and k-noise with $k = 0$ are shown in Fig. 3.

As shown in Fig. 3, for all four typical systems, H_S constantly increases with the scale or increases to the maximum value and tends to be constant. The reason for the increase of H_S is that the sampling interval lengthens with the increase of scale s (see Eq. (12)), which enhances the loss of correlations in the reconstruction of the coarse-grained time series. Among them, H_S values of the Logistic signal and the k-noise ($k = 0$) quickly turn close to their corresponding maximum values with the increase of scale s, as the coarse-grained time series becomes similar to random, therefore the maximum entropy is still maintained. That is, the increase of H_S is approximately consistent with the increase of scale, indicating the

decrease of correlations. In this case, H_S in the CECP could be regarded as an indicator of time.[23] At the same time, with the increase of scale (or the increase of H_S), the representative points of the four typical systems all evolve from R-region to N-region. But the four systems differ in their trajectories in the MS-CECP. Since different regions in the MS-CECP present different characteristics, we combine the results of MS-CECP with the corresponding coarse-grained time series (as shown in Fig. 4) to observe the changes of signal structures with the increase of scale.

It is necessary to mention that underlying correlations are responsible for the dynamical structures and constitute the deterministic behavior of a system,[23] therefore the correlations are represented by some correlational structures in the time series.

In Fig. 3(a), we can see that the trajectory of the sine signal in the MS-CECP moves from the R-region to the I-region as scale increases. Meanwhile, as shown in Fig. 4(a), the frequency of the sine signal increases with the increase of scale, but the sinusoidal structure is still held. H_S and C_{JS} values increase as the increase of frequency.

In Fig. 3(b), the trajectory of the Logistic signal moves quickly from the I-region into the N-region with the increase of scale, which indicates that the correlation decreases rapidly, quickly becoming similar to the random noise signal. From Fig. 4(b), we can see that the correlational structure of the Logistic signal, such as the structures in the red block, is lost fast as the scale increases, which accords with the results of the MS-CECP.

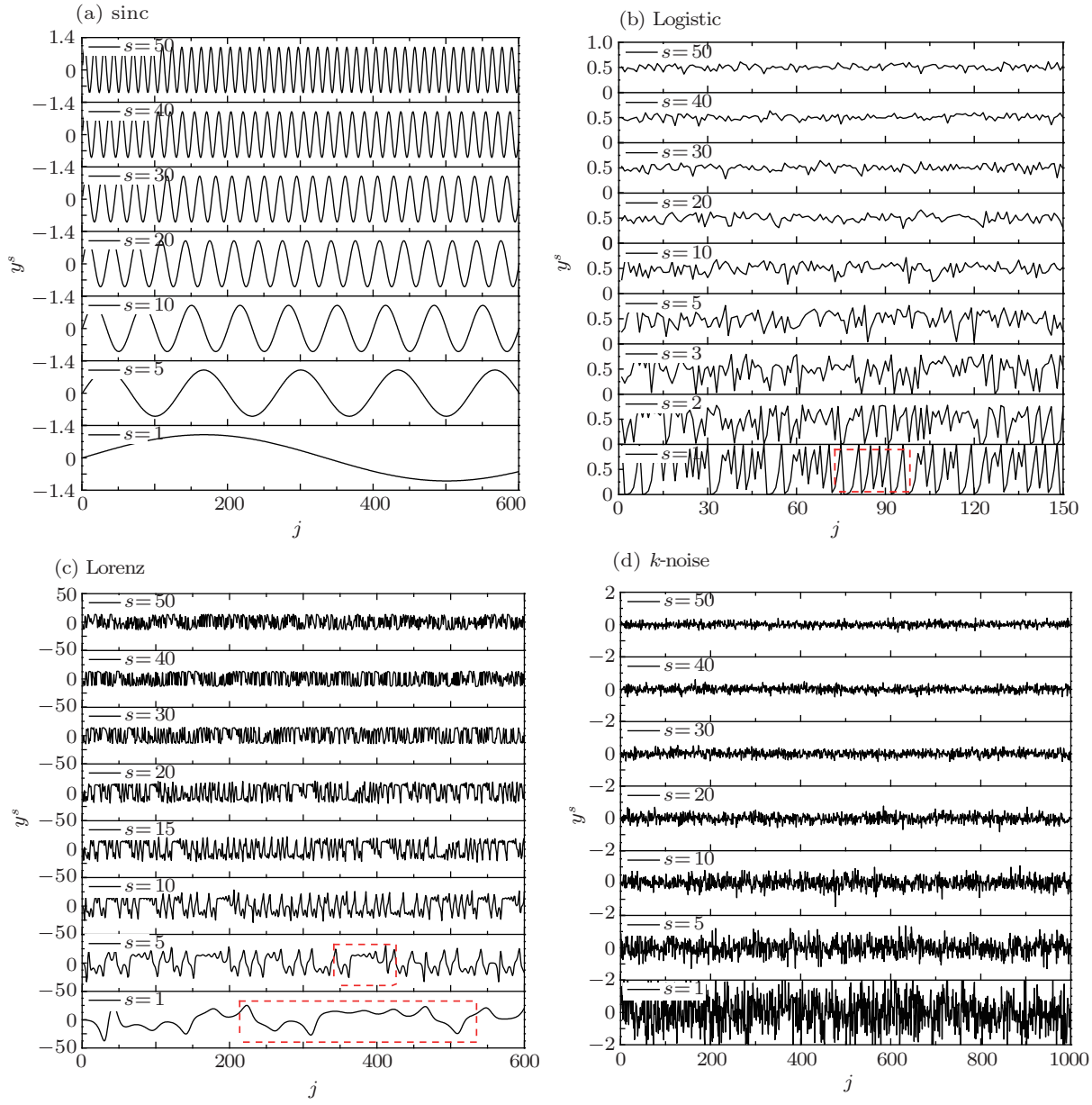


Fig. 4. (color online) Coarse-grained time series of four typical systems on different scales: (a) sine signal; (b) Logistic signal; (c) Lorenz signal; (d) k-noise ($k = 0$).

In Fig. 3(c), as the scale increases, the trajectory of the Lorenz signal first moves from the R-region to the I-region at low scales and then moves from the I-region to the N-region at high scales. Now we observe the changes of signal structures in Fig. 4(c). As scale s ranges from 1 to 10 (i.e. rising process), the coarse-grained time series for the corresponding scales still keeps the correlational structure like the original signal ($s = 1$) and increases only in frequency, which is similar to the scenario of the sine signal. On the other hand, as scale s ranges from 15 to 50 (i.e., in a decline process), the correlations decrease quickly, and the correlational structure of the coarse-grained time series becomes blurred, thereby missing the structure of the original signal ($s = 1$), which is similar to the case of the Logistic signal.

In Fig. 3(d), the results of the k-noise with $k = 0$ gather in the N-region, which is in agreement with the random feature of time series as shown in Fig. 4(d).

According to the above analyses, we find some characteristics for different regions in the MS-CECP. As the trajectory of a system in the MS-CECP moves from the R-region to the I-region (rising process) with the increase of scale, the correlational structure is lost, but it can still keep some certain structural information of the original signal, corresponding to the sine signal and the Lorenz signal at low scales. In addition, the instability of correlation structures increases with the increase of scale, reaching a maximum in the I-region. In this way, we call this process "structure keeping stage". As the scale continuously increases, the instability of correlation structures becomes so severe that they cannot hold their correlations. As a result, the correlational structures are lost quickly and fade away into the N-region which does not contain nontrivial structures, corresponding to the Logistic signal and the Lorenz signal at high scales. Thus we call this process "structure losing stage". In this way, the MS-CECP reveals the loss of the information concerning the correlational structures.

It is worth mentioning that the correlational structures constitute the hallmark of determinacy of a system.[23] Further on, we conclude that the MS-CECP reflects the determinacy of the correlational structures behind the dynamics. As the trajectory of the sine signal moves from the R-region to the I-region, it can maintain the sinusoidal structure with the increase of scale, in this way the dynamical structure of the sine signal possesses a high degree of determinacy. As located in the I-region of the CECP (Fig. 1), the Logistic signal has intricate structures with higher indeterminacy than the sine signal. As scale increases, the trajectory of the Logistic signal moves from the I-region to the N-region and the correlational structures lose quickly as a result of high indeterminacy. The Lorenz signal has a relatively high degree of determinacy at low scales but weakens at high scales. In other words, the degree of extending from the R-region to the N-region (we call it "extended degree" in the following) reflects the determinacy of a system: the lower the degree, the more deterministic the system is.

Each system has its own unique trajectory in the MS-CECP, which reflects its deterministic characteristics, so the MS-CECP can serve as an intrinsic measure for indicating the determinacy of a system.

Schuster signals with different z values exhibit different chaotic degrees, which are shown as laminar regions separated by chaotic bursts (see the red block). The size of laminar region reduces as z decreases, resulting in the enhancement of chaotic degree and the decrease of determinacy.

Figure 5 shows the MS-CECPs for Schuster maps with $z = 1.5$, 2, and 2.5, respectively. Correspondingly, we also give the coarse-grained time series of Schuster signals at different scales in Fig. 6. For $z = 2.5$, with the increase of scale, the Schuster signal is located in the R-region (Fig. 5), and can still keep clear correlational structure, which is shown as a laminar region separated by chaotic bursts (Fig. 6(c)). For $z = 2$, with the increase of scale, the trajectory in MS-CECP moves from the R-region to the I-region (Fig. 5). Although the correlational structure of the signal becomes fuzzy, some information about the initial structure is still maintained (Fig. 6(b)). For $z = 1.5$, the trajectory in MS-CECP quickly moves from the I-region into the N-region with the increase of scale (Fig. 5), and the correlational structure of signal is lost quickly (Fig. 6(a)). Consequently, the different distributions of the Schuster maps with different chaotic degrees in the MS-CECP further demonstrate that the MS-CECP can reflect the determinacy of the system.

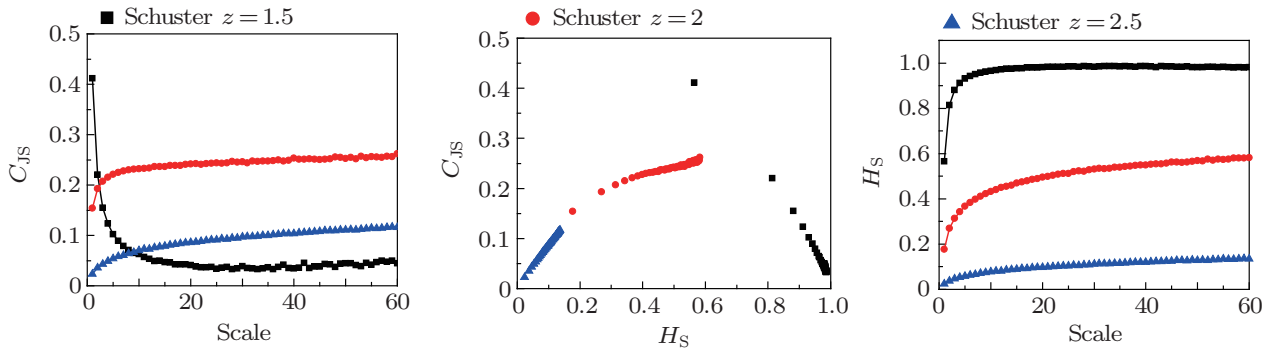


Fig. 5. (color online) MS-CECPs for Schuster maps with $z = 1.5$, 2, and 2.5.

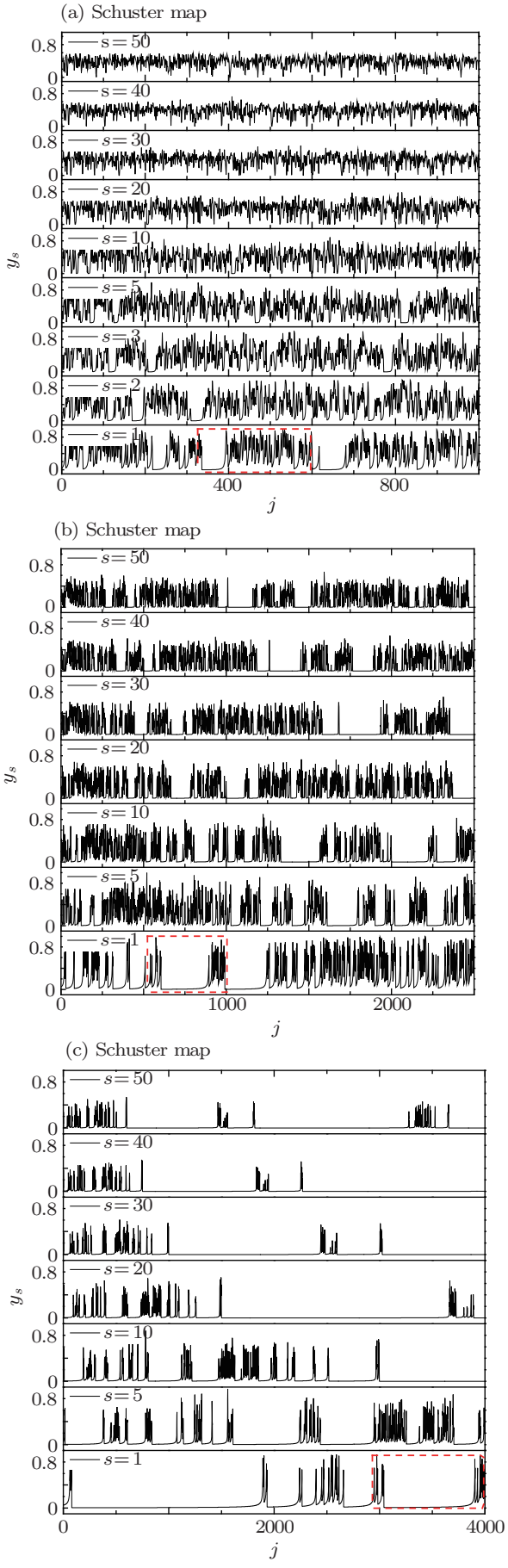


Fig. 6. (color online) Coarse-grained time series of Schuster signals at different scales: (a) $z = 1.5$; (b) $z = 2$; (c) $z = 2.5$.

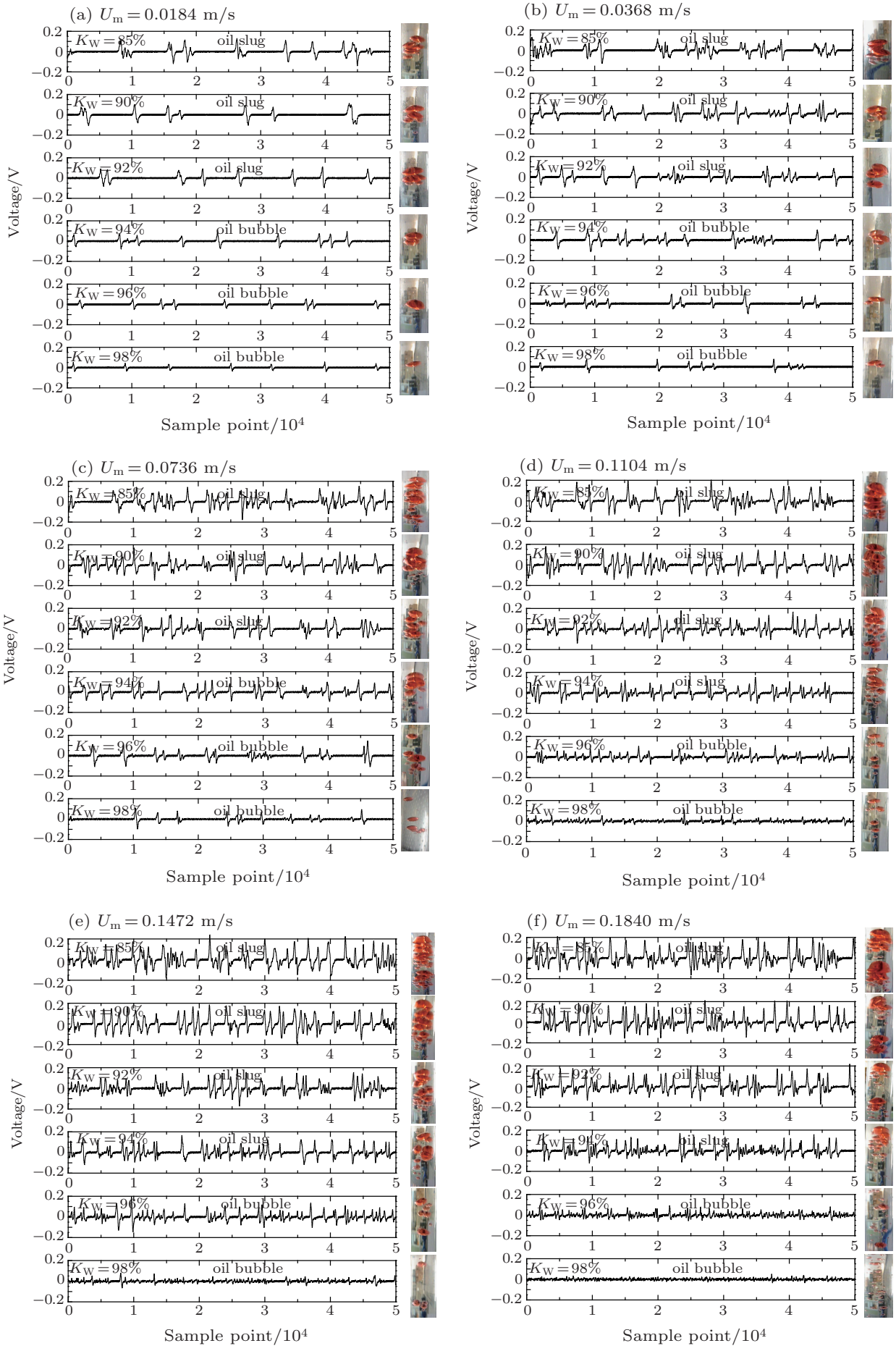
5. Multi-scale complexity entropy causality plane for two-phase flow

An oil–water two-phase flow experiment is carried out in a 20-mm diameter vertical upward transparent Plexiglas pipe in the multiphase flow loop of the Tianjin University. We fix the total oil–water flow velocity, and then change the blending ratio between water and oil phase to obtain the oil–water two-phase flow with different water volume fractions. The conductance fluctuating signals of different flow patterns are obtained by the half-ring conductance sensor,[34] which has achieved good results in the measurement of two-phase flow.[35–37] In this experiment, the values of total oil–water flow velocity $U_{\rm m}$ are 0.0184, 0.0368, 0.0736, 0.1104, 0.1472, 0.1840, 0.2208, and 0.2576 m/s and the values of water cut $K_{\rm w}$ are 85%, 90%, 92%, 94%, 96%, and 98%. The sampling frequency of conductance signal is 2 kHz, and each flow pattern records 30 seconds, collecting a total of 6×10^4 data.

Figure 7 shows the conductance fluctuating signals of vertical upward oil–water two-phase flow, which reflect the conductance characteristics of the two-phase flow. Owing to the difference in conductivity characteristic between oil and water, the amplitude of measured signal increases with the increase of oil cut through the sensor. In particular, when the test section is full of water, the voltage of the signal indicates a zero value. In order to understand the flow structure visually, we give the picture of the flow structure along with the signal.

The MS-CECP of the two-phase flow system is obtained as follows: 1) for an experimental signal, we reconstruct it by using Eq. (12), and for each scale we obtain a coarse-grained time series; 2) as shown by the method described in Section 2, we can obtain the values of both $H_{\rm S}$ and $C_{\rm JS}$ by calculating the coarse-grained time series for each scale, which corresponds to a point in the MS-CECP. In this way, we obtain the trajectory of the two-phase flow system in the MS-CECP with the increase of scale s, which describes the change of $H_{\rm S}$ and $C_{\rm JS}$ of the two-phase flow system with the increase of scale.

Due to the similarity between the chaotic signals and the experimental signals, we draw support from the MS-CECP to analyze the flow characteristics of vertical upward oil–water two-phase flow, and the results are shown in Fig. 8. In particular, the sequence length of experimental signal for calculating the MS-CECP is selected to be 5×10^4, and the maximum coarse scale is 60. From the results in Fig. 8, we can see that the trajectories in the MS-CECP are similar to those of the Lorenz signal, but different from those of the Logistic signal which moves into the N-region quickly with the increase of scale,: in this way signal length of 5×10^4 is enough to ensure an accurate result.


(a) $U_m = 0.0184$ m/s
(b) $U_m = 0.0368$ m/s
(c) $U_m = 0.0736$ m/s
(d) $U_m = 0.1104$ m/s
(e) $U_m = 0.1472$ m/s
(f) $U_m = 0.1840$ m/s
$K_W = 85\%$ oil slug
$K_W = 90\%$ oil slug
$K_W = 92\%$ oil slug
$K_W = 94\%$ oil bubble
$K_W = 96\%$ oil bubble
$K_W = 98\%$ oil bubble
Voltage/V
Sample point/10^4

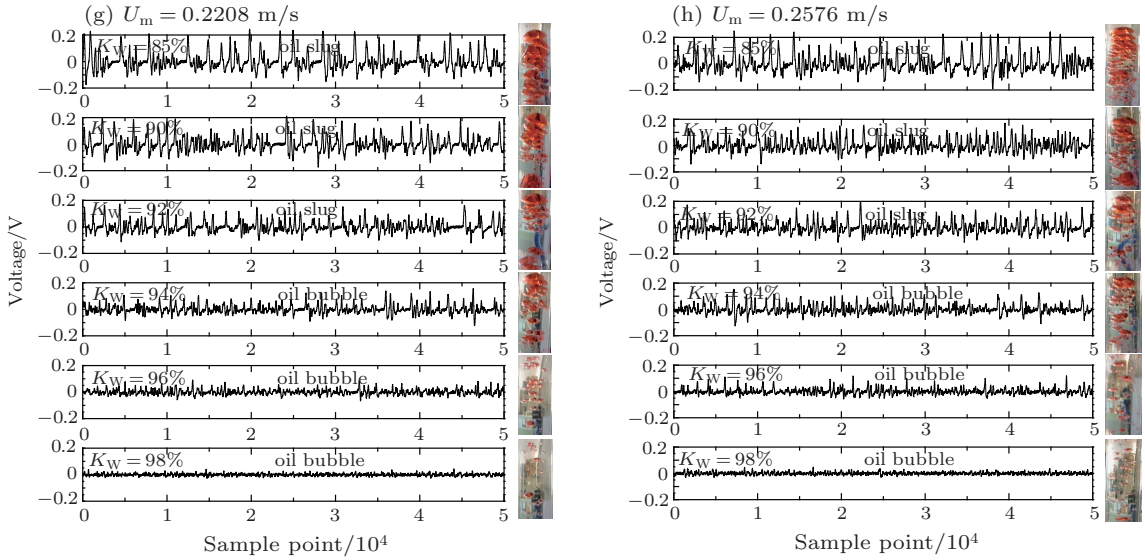


Fig. 7. (color online) Vertical upward oil-in-water flow conductance fluctuating signals with different total flow velocities and water cuts. (a) $U_m = 0.0184$ m/s, (b) $U_m = 0.0368$ m/s, (c) $U_m = 0.0736$ m/s, (d) $U_m = 0.1104$ m/s, (e) $U_m = 0.1472$ m/s, (f) $U_m = 0.1840$ m/s, (g) $U_m = 0.2208$ m/s, (h) $U_m = 0.2576$ m/s.

As can be seen in Fig. 8, with the change of total flow velocity and water volume fractions, the general shapes of the trajectories for different flow conditions are similar to each other to some degree, but different in the extension degree from the R-region to the N-region. As discussed in Section 4, the extension degree actually reflects the determinacy of the system. In this way, we then combine the oil–water two-phase signals with the corresponding flow structure (Fig. 7) to analyze the results in Fig. 8.

In the MS-CECP, the horizontal axis H_S reflects the correlation and regularity of the time series: the more irregular and random the time series, the bigger the value of H_S is. The vertical axis C_{JS} considers the perfect order process and maximal randomness process as the same complexity of zero, and the value of C_{JS} is small when the time series is periodic or stochastic. In this way, by combining C_{JS} with H_S to form the CECP, we can recognize the periodic process (in the lower left of the CECP) or stochastic process (in the lower right of the CECP) and ascertain the degree of periodicity and randomness of a system. The flow behavior of oil–water two-phase flow presents high irregularity and structural diversity, including the periodic motion of oil slugs, the stochastic motion of disperse bubbles, etc. Different flow structures contain different proportions of periodic and random behaviors which contribute to different deterministic characteristics. In this regard, the MS-CECP which can quantify the degree of period and random process is suited for distinguishing the flow behaviors of two-phase flow.

For the same total flow velocity U_m, increasing the water cut K_w causes the large oil droplets to become unstable and to break into small droplets due to the increase of turbulence energy. At low total flow velocity, the flow structures gradually transit from large oil slugs to small oil bubbles as K_w increases, which can be seen in Figs. 7(a)–7(d). However, no matter what the flow structure is, the flow behaviors all exhibit the intermittent motion of oil slugs or oil bubbles. In other words, an oil pack that is composed of oil slugs or oil bubbles is periodically repeated, followed by a liquid slug. Owing to this repetitive movement, the flow dynamic characteristic is simple and the flow behavior presents a high determinacy. Correspondingly, the results of MS-CECP in Figs. 8(a)–8(d) extend from the R-region to the I-region, to relatively lower extension degree, indicating that the flow dynamic characteristic has a high degree of determinacy. In particular, for $U_m = 0.0184$ m/s and 0.0368 m/s, when K_w values are 96% and 98%, the flow structure behaves as the intermittent motion of a single oil bubble or very few bubbles. Such a flow behavior is simpler than the flow condition with more oil bubbles or oil slug, so it obtains the lowest extended degree in the MS-CECP. In addition, when the increase of U_m, the number of oil bubbles in oil packs increases, making the determinacy of the flow structure decrease due to the irregular movements of bubbles. In this regard, the extension degree heightens slightly as the total flow velocity U_m increases.

When the total flow velocity U_m increases to 0.1472 m/s∼0.2576 m/s (Figs. 7(e)–7(h)), with the increase of K_w, breakage forces keep acting on oil droplets and the droplets become smaller and greater in number and they are separated from each other, which turns the flow structure into disperse bubble flow. Accordingly, the flow behavior is in a gradual transition from the intermittent motion of oil packs to disperse bubble flow as K_w increases, differing from the scenario from $U_m = 0.0184$ m/s∼ 0.1104 m/s. As the flow behaviors are converted from the repetitive motion of oil packs to the stochastic motion of disperse bubbles, the dynamics of flow structures become more and more indeterminate. Correspondingly, in Figs. 8(e)–8(h), with the increase of K_w, the extension degree increases continuously, which indicates that the determinacy of the flow structure is on the decrease.

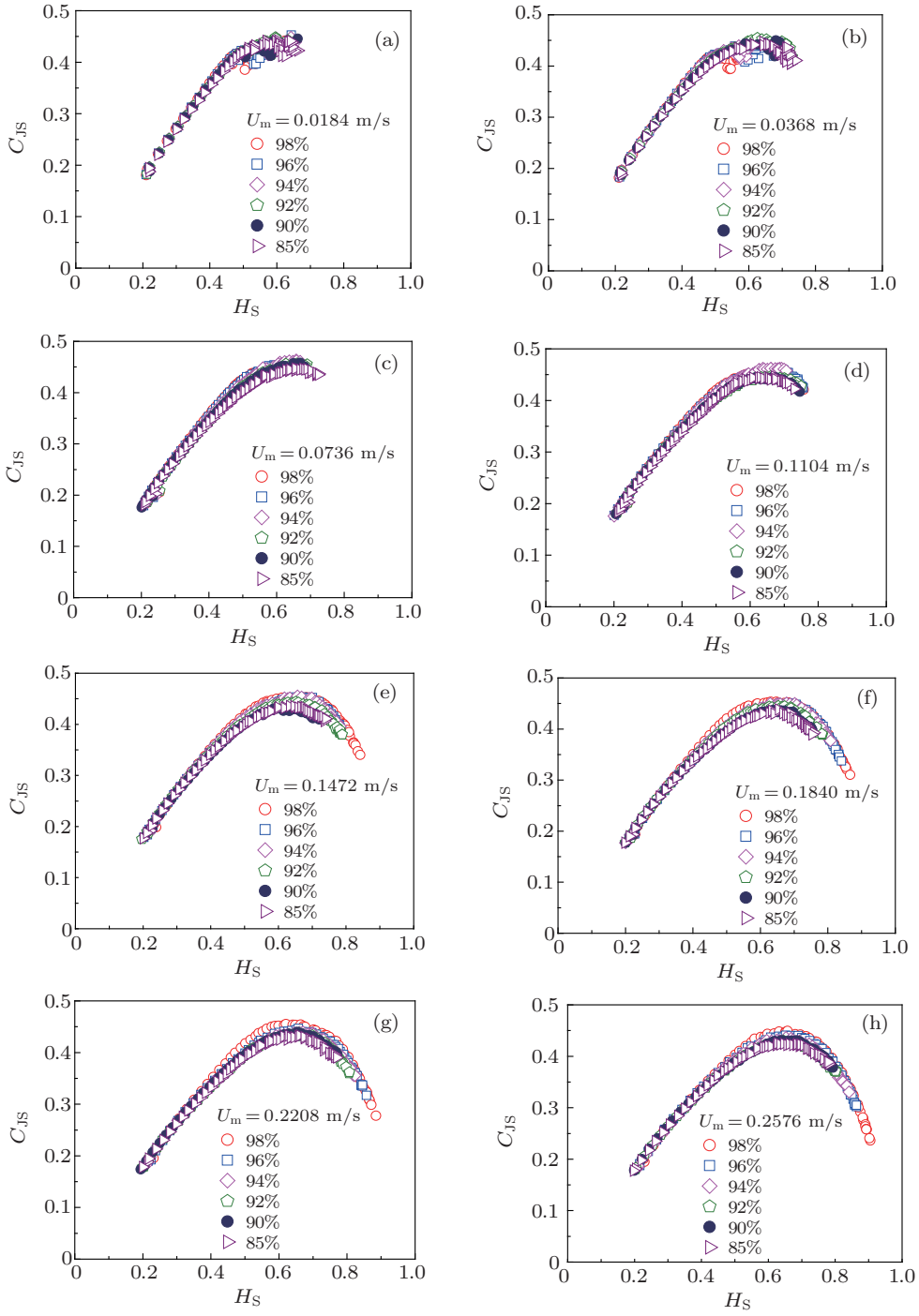


Fig. 8. (color online) MS-CECPs for vertical upward oil-in-water flow conductance fluctuating signals with different total flow velocities and water cuts. (a) $U_m = 0.0184$ m/s, (b) $U_m = 0.0368$ m/s, (c) $U_m = 0.0736$ m/s, (d) $U_m = 0.1104$ m/s, (e) $U_m = 0.1472$ m/s, (f) $U_m = 0.1840$ m/s, (g) $U_m = 0.2208$ m/s, (h) $U_m = 0.2576$ m/s.

The deterministic characteristic reflects the regular behavior of the flow structure. In the oil-in-water two-phase flow experiment, the intermittent motion of oil slugs or oil bubbles is quasi-periodic, while the stochastic motion of dispersed bubbles is irregular and random. In this way, the flow behavior of the intermittent motion of oil slugs or oil bubbles is more deterministic than that of the stochastic motion of disperse bubbles. Because of the intermittent and quasi-periodic motion of oil slugs or oil bubbles, the experimental signals present high correlations and regulations, in which H_S increases slowly with the increase of scale and C_{JS} descends slowly toward the N-region as the scale increases. Therefore, the trajectory of the MS-CECP moves slowly from the R-region to the N-region due to the strong ability of keeping this deterministic structure. On the other hand, owing to the stochastic motion of disperse bubbles, the flow behavior is

indeterminate and unpredictable, therefore H_S increases fast with the increase of scale and C_{JS} descends quickly toward the N-region as the coarse-grained time series become more and more random with the increase of scale. Hence, the trajectory of the MS-CECP moves quickly from the R-region into the N-region. When fixing the total flow velocity U_m and gradually increasing the water fraction K_w, the flow structure gradually transforms from the intermittent motion of oil slugs or oil bubbles to the stochastic motion of dispersed oil bubbles, and in this process the degree of deterministic characteristic of the flow structure decreases gradually. As the flow behavior becomes more and more irregular and unpredictable, the growth rate of H_S becomes rapid and the descending degree of C_{JS} increases toward the N-region. Therefore, the trajectory of the MS-CECP moves more and more quickly from the R-region to the N-region as the flow structure gradually transforms from the intermittent motion of oil slugs or oil bubbles into the stochastic motion of dispersed oil bubbles. Correspondingly, the extension degree of the trajectory from the R-region to the N-region in the MS-CECP becomes higher and higher with the increase of K_w. In this regard, the MS-CECP can clearly reflect the difference in determinacy between the flow structures in this transient process. As a consequence, the above results suggest that the MS-CECP can detect the deterministic characteristics of different flow patterns.

6. Conclusions

The CECP, which is regarded as a measure of complexity induced by the correlational structure, can quantify the degree of periodicity unpredictable and further detect intricate structures or patterns behind the dynamics. To better characterize the dynamic characteristics of a system, we combine the CECP with the multi-scale method to propose the MS-CECP. Through the analysis of several typical dynamic systems, we find that the MS-CECP reveals the loss of the information of a typical dynamical system and can reflect the determinacy of the system. We use the MS-CECP to investigate the oil-in-water two-phase flow and find that the MS-CECP can detect the deterministic characteristics of different flow patterns. Our results suggest the MS-CECP could be an intrinsic measure for indicating two-phase flow structures.

References

[1] Daw C S, Finney C E A, Vasudevan M, van Goor N A, Nguyen K, Bruns D D, Kostelich E J, Grebogi C, Ott E and Yorke J A 1995 *Phys. Rev. Lett.* **75** 2308
[2] Fan L T, Neogi D, Yashima M and Nassar R 1990 *AIChE J.* **36** 1529
[3] van Ommen J R, Coppens M O, van den Bleek C M and Schouten J C 2000 *AIChE J.* **46** 2183
[4] Li H W, Zhou Y L, Wang S Y and Sun B 2013 *Acta Phys. Sin.* **62** 140505 (in Chinese)
[5] Cao Y, Wang J, He Y, Liu W and Yang Y 2009 *AIChE J.* **55** 3099
[6] La Forgia N, Fernandino M and Dorao C A 2014 *Heat Transfer Engineering* **35** 440
[7] Komrakova A E, Shardt O, Eskin D and Derksen J J 2014 *Int. J. Multiphase Flow* **59** 24
[8] Zhang N, Yao J, Huang Z Q and Wang Y Y 2013 *J. Comput. Phys.* **242** 420
[9] Jones O C Jr and Zuber N 1975 *Int. J. Multiphase Flow* **2** 273
[10] Song C H, No H C and Chung M K 1995 *Int. J. Multiphase Flow* **21** 381
[11] Sun B, Wang E P and Zheng Y J 2011 *Acta Phys. Sin.* **60** 014701 (in Chinese)
[12] Du M, Jin N D, Gao Z K, Wang Z Y and Zhai L S 2012 *Int. J. Multiphase Flow* **41** 91
[13] Jones J O C and Zuber N 1975 *Int. J. Multiphase Flow* **2** 273
[14] Song C H, No H C and Chung M K 1995 *Int. J. Multiphase Flow* **21** 381
[15] Daw C S, Finney C E A, Vasudevan M, van Goor N A, Nguyen K, Bruns D D, Kostelich E J, Grebogi C, Ott E and Yorke J A 1995 *Phys. Rev. Lett.* **75** 2308
[16] Gandhi A B, Joshi J B, Kulkarni A A and Jayaraman V K 2008 *Int. J. Multiphase Flow* **34** 1099
[17] Wang Z Y, Jin N D, Gao Z K, Zong Y B and Wang T 2010 *Chem. Eng. Sci.* **65** 5226
[18] Gao Z K, Zhang X W, Du M and Jin N D 2013 *Phys. Lett. A* **377** 457
[19] Zheng G B and Jin N D 2009 *Acta Phys. Sin.* **58** 4485 (in Chinese)
[20] Fan C L, Jin N D, Chen X T and Gao Z K 2013 *Chin. Phys. Lett.* **30** 090501
[21] Lopez–Ruiz R, Mancini H L and Calbet X 1995 *Phys. Lett. A* **209** 321
[22] Martín M T, Plastino A and Rosso O A 2003 *Phys. Lett. A* **311** 126
[23] Lamberti P W, Martín M T, Plastino A and Rosso O A 2004 *Physica A* **334** 119
[24] Rosso O A, Larrondo H A, Martin M T, Plastino A and Fuentes M A 2007 *Phys. Rev. Lett.* **99** 154102
[25] Zunino L, Fernández Bariviera A, Guercio M B, Martinez L B and Rosso O A 2012 *Physica A* **391** 4342
[26] Zunino L, Tabak B M, Serinaldi F, Zanin M, Pérez D G and Rosso O A 2011 *Physica A* **390** 876
[27] Ribeiro H V, Zunino L, Mendes R S and Lenzi E K 2012 *Physica A* **391** 2421
[28] Crutchfield J P and Young K 1989 *Phys. Rev. Lett.* **63** 105
[29] Grassberger P 1986 *Int. J. Theor. Phys.* **25** 907.
[30] Shiner J S, Davison M and Landsberg P T 1999 *Phys. Rev. E* **59** 1459
[31] Bandt C and Pompe B 2002 *Phys. Rev. Lett.* **88** 174102
[32] Kennel M B, Brown R and Abarbanel H D I 1992 *Phys. Rev. A* **45** 3403
[33] Costa M, Goldberger A L and Peng C K 2002 *Phys. Rev. Lett.* **89** 068102
[34] Gao Z K, Hu L D, Zhou T T and Jin N D 2013 *Acta Phys. Sin.* **62** 110575 (in Chinese)
[35] Kytömaa H K, Brennen C E 1991 *Int. J. Multiphase Flow* **17** 13
[36] Costigan G and Whalley P B 1997 *Int. J. Multiphase Flow* **23** 263
[37] Cantelli L, Fichera A and Pagano A 2011 *J. Thermodyn.* **2011** 491350